Solid State and Solution Conformation of [Ala^7]-Phalloidin: A Synthetic Phallotoxin Analogue

Giancarlo Zanotti,[b] Lucia Falcigno,[a, c] Michele Saviano,[c] Gabriella D'Auria,[a, c] Bianca Maria Bruno,[b] Tiziano Campanile,[a] and Livio Paolillo*[a]

Dedicated to the memory of Professor Theodor Wieland

Abstract: Phallotoxins are toxic compounds produced by poisonous mushroom *Amanita phalloides* and belong to the class of bicyclic peptides with a transannular thioether bridge. Their intoxication mechanism in the liver involves a specific binding of the toxins to F-actin that, consequently, prevents the depolymerization equilibrium with G-actin. Even though the conformational features of phallotoxins have been worked out in solution, the exact mechanism of interaction with F-actin is still unknown. In this study a toxic phalloidin synthetic derivative, bicyclo(Ala^1-D-Thr^2-Cys^3-*cis*-4-hydroxy-Pro^4-Ala^5-2-mercapto-Trp^6-Ala^7)(S-3 → 6) has been synthesized. A substitution at position 7, with an Ala residue replaces the 4,5-dihydroxy-Leu present in the natural phalloidin. This analogue has formed crystals suitable for X-ray analysis, and represents the first case for such a class of compounds. The solid-state structure as well as the solution conformation have been evaluated. NMR techniques have been used to extract interproton distances as restraints in subsequent molecular dynamics calculations. Finally, a direct comparison between structures in solution and in the solid state is presented.

Keywords: NMR spectroscopy · peptides · phallotoxin analogue · X-ray diffraction

Introduction

Amanita phalloides and *Amanita verna* are mushrooms with lethal toxicity. They contain the following three main families of toxic cyclopeptides namely amatoxins, virotoxins, and phallotoxins.[1] Phallotoxins are bicyclic heptapeptides, characterized by a thioether bridge between cysteine and tryptophan side chains and by the presence of uncommon hydroxylated amino acids. Phalloidin, the main component of phallotoxins, was obtained as a pure crystalline product by Lynen and Wieland.[2] The other components of the phallotoxin family were later isolated and characterized.[3–5] The general formula and the chemical structure of naturally occurring phallotoxins are reported in Figure 1 and Table 1,

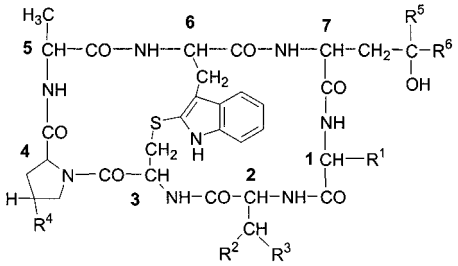

Figure 1. General formula of phallotoxins. The different substituents are listed in Table 1.

respectively. Phallotoxins are quick acting poisons, since they cause death in the treated animals 2–5 hours after intraperitoneal injection. Nevertheless, phallotoxins do not seem to play any role in the lethal mushroom poisoning of humans,

[a] Prof. Dr. L. Paolillo, Dr. L. Falcigno, Dr. G. D'Auria, Dr. T. Campanile
Dipartimento di Chimica, Università di Napoli "Federico II"
Complesso Universitario Monte S. Angelo
via Cintia 80126, Napoli (Italy)
E-mail: paolillo@chemistry.unina.it

[b] Dr. G. Zanotti, Dr. B. M. Bruno
Centro di Chimica del Farmaco del CNR
Università di Roma "La Sapienza", Piazzale A. Moro, Roma (Italy)

[c] Dr. L. Falcigno, Dr. M. Saviano, Dr. G. D'Auria
Centro di Studio di Biocristallografia del C.N.R.
Università di Napoli "Federico II"
Via Mezzocannone, 4 80134, Napoli (Italy)
Fax: (+39) 081-674090

Supporting information for this article is available on the WWW under http://www.wiley-vch.de/home/chemistry/ or from the author. Supporting Information available (16 pages): Synthesis protocol and schemes (five pages). Tables from the X-ray analysis of atomic coordinates (Table S1), bond lengths and angles (Table S2), anisotropic displacement parameters (Table S3), torsion angles (Table S4). Tables of ^{13}C NMR shifts (Table S5) and experimental ϕ angles evaluated by means of the Karplus equation (Table S6) from NMR analysis. Proton–proton distances (Table S7) from NMR data and MD calculations.

  0947-6539/01/0707-1479 $ 17.50+.50/0

Table 1. Naturally occurring phallotoxins.

Compound	R^1	R^2	R^3	R^4	R^5	R^6
phalloin	CH_3	CH_3	OH	OH	CH_3	CH_3
phalloidin	CH_3	CH_3	OH	OH	CH_2OH	CH_3
phallisin	CH_3	CH_3	OH	OH	CH_2OH	CH_2OH
prophalloin	CH_3	CH_3	OH	H	CH_3	CH_3
phallacin	$CH(CH_3)_2$	OH	COOH	OH	CH_3	CH_3
phallacidin	$CH(CH_3)_2$	OH	COOH	OH	CH_2OH	CH_3
phallisacin	$CH(CH_3)_2$	OH	COOH	OH	CH_2OH	CH_2OH

since these compounds are not absorbed in the gastrointestinal tract.

The toxic effect of phallotoxins is closely related to their capacity to bind strongly F-actin.[6, 7] Actin, a class of important ubiquitous proteins of about 43 kDa, exist in an equilibrium of a monomeric form, G-actin, and a polymeric one, called F-actin. Phallotoxins accelerate the polymerization process with an about 30-fold F-actin increment in the equilibrium G-actin $\rightleftharpoons$ F-actin. By conjugation with phallotoxins, F-actin filaments are highly stabilized against chemical and physical depolymerization agents[8, 9] and resistant to heat denaturation and proteolytic degradation.[10]

Conformational studies carried out on natural phallotoxins and on active and inactive analogues can afford useful information on the still unknown molecular mechanism of the binding to F-actin. The conformation of phallotoxins has been studied only by NMR techniques[11–15] because so far no crystal structure of phallotoxins has been obtained. Indeed, phalloidin and its derivatives crystallize in very thin, asbestos-like fibers, not suitable for X-ray analysis.

In this paper we report on the crystal and molecular structure of bicyclo(Ala^1-D-Thr^2-Cys^3-*cis*-4-hydroxy-Pro^4-Ala^5-2-mercapto-Trp^6-Ala^7)(S-3 $\rightarrow$ 6), namely [Ala^7]-phalloidin. This toxic synthetic derivative is modified at position 7, where the L-Ala^7 replaces the 4,5-dihydroxy-L-Leu^7 residue present in the natural phalloidin. [Ala^7]-phalloidin is about six times less active than phalloidin in the F-actin binding. The bioactivity was measured as the ability of the analogue to displace [^{3}H]-dimethylphalloidin from its binding complex with F-actin. The solution structure of the analogue obtained by two-dimensional NMR spectroscopy in [D_6]dimethyl sulfoxide (DMSO) and molecular dynamics calculations are also described. Solid-state and solution structures will be shown to be almost identical.

Results and Discussion

Synthesis: The synthesis of [Ala^7]-phalloidin has been carried out by the classical method in solution by adopting the Savige – Fontana approach to establish the cross-link thioether bridge. This method is based on the use of the oxidation derivative of tryptophan-L-3a-hydroxy-1,2,3,3a,8,8a-hexahydropyrrolo[2,3-*b*]indole-2-carboxylic acid (Hpi).[16] Under acidic conditions, this compound forms a 2-thioindolyl ether bond with thiol groups.[17, 18] This method has already been applied to the synthesis of amatoxin and phallotoxin analogues.[19–21]

The linear heptapetide precursor is equipped solely with acid-labile protecting groups. The N- and C-terminal Hpi and alanine residues are protected with the *tert*-butyloxycarbonyl (Boc) groups and as *tert*-butylester (O*t*Bu), respectively, while the triphenylmethyl (Trt) and *tert*-butyl ether (*t*Bu) groups have been chosen to protect the side chains of the cysteine and threonine residues. On treatment with trifluoroacetic acid (TFA) all of the groups mentioned above are split off with the simultaneous formation of the sulfur bridge to give the monocyclic thioether peptide, which thereafter can be cyclized to the final phalloidin analogue. Detailed synthesis information is available as Supporting Information.

The CD spectrum of [Ala^7]-phalloidin corresponds to that of phalloidin with positive Cotton effects around 240 and 300 nm.[22]

The mass spectrum measurement (FAB) of $[M - H]^+$ shows a mass of 715 a.m.u. as expected.

X-ray analysis: The molecular model of [Ala^7]-phalloidin, as derived from the solid-state analysis, is shown in Figure 2. All amino acid residues are in the L-configuration, with the exception of the D-Thr^2. The geometrical parameters for all residues are close to the expected values.[23, 24] The molecule presents all peptide bonds in a *trans*-configuration, with values ranging between 168 – 180° and with an average value of 171°. The large macrocyclic heptapeptide ring of 21 atoms is "bent" at the bridging points. The bridging segment of five atoms (containing the indole ring and the thioether group) participates in two rings, a 15-membered ring (ring 1) and an 18-membered ring (ring 2). Ring 1 contains the backbone of residues 4 and 5, while ring 2 contains the backbone of the residues 1, 2, and 7. The planes of the two rings form dihedral angles of about 90.0(5)°. The indole ring lies approximately in the plane of ring 1, containing the *cis*-4-hydroxy-4-proline

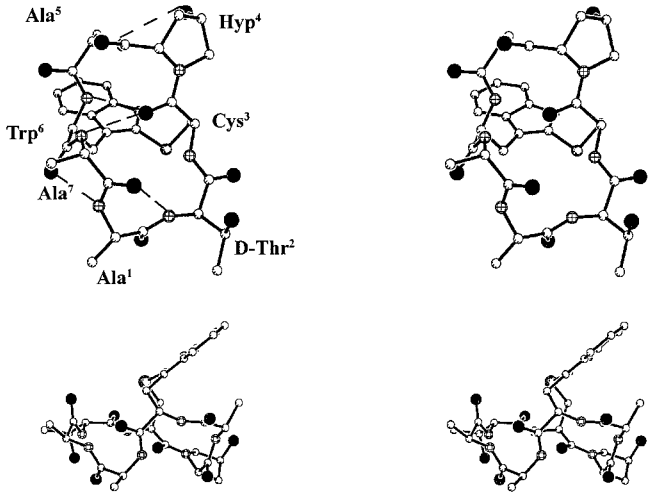

Figure 2. Stereodrawing of the molecular model of [Ala^7]-phalloidin as obtained from X-ray analysis as viewed almost along the *a* axis (top) and almost along the *b* axis (bottom). The intramolecular hydrogen bonds are indicated as dashed lines.

0947-6539/01/0707-1480 $ 17.50+.50/0 *Chem. Eur. J.* **2001**, *7*, No. 7

Table 2. Intra- and intermolecular hydrogen bonds of [Ala7]-phalloidin crystal structure.

Donor	Acceptor	Distance [Å] H···O	D···A	Angle [°] D-H···A	N···O=C′	
Intramolecular						
N_1	O_6	2.03	2.831(4)	154.9	89.1(2)	
N_2	O_7	2.23	2.970(4)	144.7	93.1(2)	
N_5	O^{γ}_4	2.48	3.074(4)	126.1	99.4(2)	
N_6	O_3	2.24	3.020(4)	150.3	121.5(2)	
N_7	O_3	2.39	2.907(4)	119.4	176.3(2)	
Donor	Acceptor	Distance [Å] H···O	D···A	Angle [°] D-H···A	N···O=C′	Symmetry operation
Intermolecular						
O^{γ}_2	O^{γ}_4	2.34	2.725(4)	109.3	124.8(2)	$-\frac{1}{2}+x, \frac{1}{2}-y, 1-z$
O^{γ}_4	O_5	1.86	2.661(3)	164.6	145.5(2)	$1-x, \frac{1}{2}+y, \frac{1}{2}-z$
$N^{\varepsilon}{}_6$	O_2	2.08	2.915(4)	164.8	108.5(2)	$\frac{1}{2}+x, \frac{1}{2}-y, 1-z$

(Hyp4)-Ala5 residues and giving rise to an overall distorted "T" shape of the molecule.

All potential donor groups NH and OH are involved in hydrogen bonds except the Cys3-NH. Details on intra- and intermolecular hydrogen bonds of the [Ala7]-phalloidin crystal structure are listed in Table 2. The backbone conformation of [Ala7]-phalloidin is stabilized in the solid state by the following hydrogen bonds:

i) an intramolecular $4 \rightarrow 1$ hydrogen bond, between the Trp6-NH and the Cys3-CO, with a type I β-turn formation;
ii) an intramolecular $5 \rightarrow 1$ hydrogen bond between the Ala7-NH and the Cys3-CO, with the formation of a α-turn of type Ia;[25]
iii) an intramolecular $3 \rightarrow 1$ hydrogen bond, between the Ala1-NH and the Trp6-CO, with an equatorial γ-turn formation;
iv) an intramolecular $3 \rightarrow 1$ hydrogen bond, between the D-Thr2-NH and the Ala7-CO, leading to an axial γ-turn;
v) an intramolecular hydrogen bond between the Ala5-NH and the Hyp4-O^{γ}_4.

In Table 3 the solid state torsion angles for [Ala7]-phalloidin are summarized. All values for the ϕ and ψ angles fall within the allowed regions of the Ramachandran map.

The D-Thr2 side chain has $\chi^{1,1}$ and $\chi^{1,2}$ values close to 60° (g^+ conformation) and −60° (g^- conformation), respectively. This corresponds to one of the stable conformations for this residue in a D-configuration.[24]

The Hyp4 residue, characterized by positive χ^1 and χ^3 values and negative χ^2 and χ^4 values, adopts a $C^{s\gamma}$-*endo*-type conformation.[26]

The indole ring of the Trp6 presents structural parameters similar to those found in nonbridging indole structures and in the isolated amino acid.[27, 28] The Trp6 side chain has χ^1, $\chi^{2,1}$, and $\chi^{2,2}$ values of −38.8°, 120.1° and −56.1°, respectively. This conformation is slightly different from the more common observation of −60° and 90° in proteins and 60° and 90° in small molecules.[28] This deviation from the minimum energy conformations is very likely owing to the bridging effect. By analogy, the Cys3 side chain (the other side of the bridge) is forced into the uncommon conformational χ^1 angle of 28.6°.[29]

The molecules in the solid state are held together by a network of hydrogen bonds, as described in Table 2. All distances of the type N-H···O and O-H···O are within expected values.[30] In the crystal the molecules are held together by O^{γ}_2-H···O^{γ}_4 and N^{ε}_6–H···O_2 intermolecular hyrogen bonds, with the formation of rows of symmetry related molecules aligned along the *a* direction. These rows are linked together along the *c* direction by one intermolecular hydrogen bond between the Hyp4-O^{γ}_4-H and the Ala5-CO. The structure is further stabilized by van der Waals contacts.

Detailed structural parameters are available as Supporting Information.

NMR analysis: Proton resonances were assigned with the aid of TOCSY,[31] DQF-COSY,[32, 33] ROESY[34, 35] and NOESY[36, 37] spectra, and aliphatic and aromatic carbon resonances by HMQC experiments.[38–40]

All proton spin systems were identified in the TOCSY spectrum at a mixing time of 70 ms. D-Thr2 and Hyp4 residues were easily identified from their coupling patterns. The sequential assignment of the Cys3 and Trp6 AMX systems and of the three alanine spin systems was achieved by exploitation of the interresidue $H^{\alpha}(i) \leftrightarrow NH(i+1)$, $NH(i) \leftrightarrow NH\ (i+1)$ NOE effects and $H^{\alpha}(i) \leftrightarrow H^{\delta}(i+1)$ NOE in the case of Cys3–Hyp4.[41] Table 4 shows the complete assignment of the proton resonances. Prochiral protons were stereospecifically assigned from the intraresidue NOE effects such as $H^{\beta} \leftrightarrow NH$ or $H^{\beta} \leftrightarrow H^{\alpha}$ and the $^3J(H^{\alpha},H^{\beta})$ coupling constants, obtained from either ^1H or DQF-COSY spectra.

The protonated carbons were identified in the HMQC spectrum from the chemical shifts of the directly bound protons. Carbon chemical shifts are available as Supporting Information.

The conformational analysis of [Ala7]-phalloidin is based on the $^3J(H,H)$ coupling constants, the temperature dependence of the NH protons and ROE effects. Most $^3J(NH,H^{\alpha})$ couplings were taken directly from the ^1H NMR spectrum. Cys3 and Ala5 $^3J(NH,H^{\alpha})$ were measured from the DQF-COSY spectrum since both NH resonances overlap with the

Table 3. Torsion angles in degrees of [Ala7]-phalloidin as obtained from X-ray analysis.[a]

Residue	ϕ	ψ	ω	χ^1	$\chi^{1,1}$	$\chi^{1,2}$	χ^2	$\chi^{2,1}$	$\chi^{2,2}$	χ^3	χ^4
Ala1	−86.5(4)	75.5(4)	168.6(3)								
D-Thr2	121.3(3)	−7.4(4)	−170.5(3)		61.6(4)	−60.7(4)					
Cys3	−169.5(3)	152.7(3)	−171.0(3)	28.6(4)							
Hyp4	−64.2(4)	−35.6(4)	−179.5(3)	19.4(4)			−35.0(4)			36.4(4)	−25.8(4)
Ala5	−72.4(4)	−19.9(5)	−168.3(3)								
Trp6	−111.3(4)	−13.8(4)	−168.0(3)	−38.8(4)				120.1(4)	−56.1(4)		
Ala7	71.2(4)	−59.5(4)	−173.1(3)								

[a] C^{α}_3-C^{β}_3-S^{γ}_3-$C^{\delta 2}_6$: 112.3(3); $C^{\delta 1}_6$-C^{γ}_6-$C^{\delta 2}_6$-$S^{\gamma 2}_3$: −169.8(3); C^{β}_6-C^{γ}_6-$C^{\delta 2}_6$-S^{γ}_3: 13.3(5); C^{β}_3-S^{γ}_3-$C^{\delta 2}_6$-$C^{\gamma 2}_6$: −120.3(3); C^{β}_3-S^{γ}_3-$C^{\delta 2}_6$-N^{ε}_6: 71.0(3).

Table 4. ^{1}H NMR shifts of [Ala^7]-phalloidin in [D$_6$]DMSO at 298 K.

Xxx	NH	H$^\alpha$	H$^\beta$	H$^\gamma$	others
Ala^1	7.32	4.47	1.21		
D-Thr^2	8.50	3.96	4.24	1.06	OH 4.77
Cys^3	7.69	4.73	3.51$^{pro\text{-}R}$		
			3.22$^{pro\text{-}S}$		
Hyp^4		4.14	2.29	4.33	OH$^\gamma$ 5.47
			1.18		H$^\delta$ 3.51, 3.76
Ala^5	7.70	3.90	0.79		
Trp^6	7.26	4.81	3.11$^{pro\text{-}R}$		H′$_4$ 7.70, H′$_5$ 6.98, H′$_6$ 7.10
			3.32$^{pro\text{-}S}$		H′$_7$ 7.23, NH$_{ind}$ 11.20
Ala^7	8.48	3.87	1.15		

Trp^6–H′$_7$ signal. The other ^3J coupling constants were also measured from the DQF-COSY spectrum and are collected in Table 5.

The temperature dependence of the NH and O$^\gamma$H protons (for D-Thr^2 and Hyp^4) were obtained from ^{1}H NMR spectra recorded between 298 and 310 K (Table 6). Owing to overlap

Table 5. Vicinal coupling constants [Hz] of [Ala^7]-phalloidin.

^3J [Hz]	Ala^1	D-Thr^2	Cys^3	Hyp^4	Ala^5	Trp^6	Ala^7
NH,H$^\alpha$	7.1	7.6	7.5		7.3	9.7	5.1
H$^\alpha$,H$^{\beta pro\text{-}R}$	6.5	2.9	6.0	5.8[a]	7.3	6.0	6.5
H$^\alpha$,H$^{\beta pro\text{-}S}$			7.2	8.4[a]		11.0	

[a] Stereospecific assignment is ambiguous.

Table 6. Temperature dependence of the NH chemical shifts $\Delta\delta/\Delta T$ [ppb K^{-1}] of [Ala^7]-phalloidin in [D$_6$]DMSO.

	Ala^1	D-Thr^2	Cys^3	Ala^5	Trp^6	Ala^7
$-\Delta\delta/\Delta T$	4.0	6.6	0.93	3.7	3.4	6.2

of the Cys^3-NH and Ala^5-NH resonances, relative temperature coefficients were estimated from TOCSY spectra in the same temperature range. As shown in Table 6, relatively small temperature coefficients can be noted for Cys^3-NH (-0.93 ppb K^{-1}) and Trp^6-NH (-3.4 ppb K^{-1}) and also for D-Thr^2–O$^\gamma$H (-2.5 ppb K^{-1}). These data indicate that these protons can be involved in hydrogen bonding.

Structure refinement by molecular dynamic calculations: Interproton distances computed by cross-relaxation rate values evaluated from ROESY spectra (σ^R) were used in energy minimization (EM) and molecular dynamic (MD) simulations, as they are more reliable for a correlation time (τ_c) in the nanosecond range.[42] Interproton distances are available as Supporting Information.

The molecular model averaged over the last 50 ps of restrained vacuum MD calculations, namely A7PHV, is shown in Figure 3.

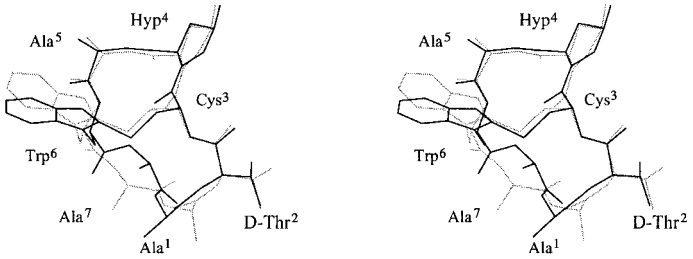

Figure 3. A stereoview of the backbone superposition of the average molecular models: A7PHV (black line) and A7PHW (grey line).

The experimental NMR data are well represented in the calculations. The backbone dihedral angles, averaged over the last 50 ps of the restrained MD calculations (Table 7) are in good agreement with the experimental ϕ values, derived from the Karplus-type equation of Bystrov[43] (data available as Supporting Information). It should be noted that the occurrence of a type I β-turn in the Cys^3-Hyp^4-Ala^5-Trp^6 segment is indicated by the dihedral angles (ϕ Hyp^4 $= -45.9$, ψ Hyp^4 $= -33.4$, ϕ Ala^5 $= -71.0$, ψ Ala^5 $= -24.6$) which are in accord with those regularly found in such turns.[44] The experimental distances Ala^{5}NH–Trp^{6}NH (2.4 Å) and Ala^{5}NH–Hyp^{4}H$^\alpha$ (3.2 Å) are, also, in good agreement with the type I β-turn hypothesis. The turn also appears to be stabilized by a hydrogen bond between the Cys^{3}CO and the Trp^{6}NH, and explains the small $\Delta\delta/\Delta T$ value of the Trp^{6}NH proton (Table 6).

ROE distance restraints correlate globally with the exception of the Ala^{7}NH–Trp^{6}H$^\alpha$ distance (3.2 Å instead of the experimental 2.5 Å). All other calculated distances are strikingly similar within the limits of the estimated deviations.

As seen from Figure 3 the Ala^5-methyl group lies in the anisotropy area of the Trp^6 indole system, a result which is in agreement with the high-field shift of the Ala^5-methyl resonance (Table 4).

In order to check the stability of this structure, the average model A7PHV has been minimized using EM with the conjugate gradients algorithm and then it has been incorporated in a box of 300 water molecules. A MD calculation in water was then performed at 300 K for 110 ps. The trajectory from 60 ps to 110 ps has been used for statistical analysis.

The molecular model averaged over the last 50 ps of unrestrained MD calculations in water, namely A7PHW, shown in Figure 3, is very close to A7PHV calculated with restrained MD in vacuo. The root-mean-square-deviation

Table 7. Backbone angles [°] averaged during the last 50 ps MD calculations (A7PHV = average structure from rMD in vacuum, A7PHW average structure from MD in water). The values in parentheses are the RMSD in degrees.

Residue	A7PHV			A7PHW		
	ϕ	ψ	ω	ϕ	ψ	ω
Ala^1	-118.0	61.8	169.6	-119.6 ($\pm$23.3)	130.1 ($\pm$17.7)	164.0 ($\pm$40.5)
D-Thr^2	97.8	-34.9	-170.6	102.7 ($\pm$16.6)	-86.8 ($\pm$11.1)	-167.0 ($\pm$19.8)
Cys^3	-95.9	127.2	175.3	-70.7 ($\pm$11.2)	135.1 ($\pm$13.6)	166.3 ($\pm$30.6)
Hyp^4	-45.9	-33.4	-169.3	-50.4 ($\pm$9.7)	-40.9 ($\pm$12.4)	-169.4 ($\pm$36.2)
Ala^5	-71.0	-24.6	169.6	-80.4 ($\pm$22.9)	-7.1 ($\pm$34.3)	170.9 ($\pm$3.8)
Trp^6	-100.5	-22.4	-166.6	-106.7 ($\pm$16.6)	-84.4 ($\pm$34.2)	-169.8 ($\pm$9.3)
Ala^7	65.0	2.9	-165.1	-135.3 ($\pm$60.6)	-70.5 ($\pm$17.3)	167.6 ($\pm$5.0)

0947-6539/01/0707-1482 $ 17.50+.50/0 *Chem. Eur. J.* **2001**, *7*, No. 7

(RMSD) between the A7PHW and A7PHV models is 0.68 Å for the backbone, including the oxygens and the thioether bridge.

In both A7PHW and A7PHV molecular models a type I β-turn occurs in the Cys^3-Hyp^4-Ala^5-Trp^6 segment as indicated from the ϕ- and ψ-dihedral angles (Table 7). This region, with the sulfide bridge essential for the toxicity of the molecule, appears very rigid throughout the MD simulation, whilst larger flexibility is observed in the other part of the molecule (Ala^7 to D-Thr^2) known to be nonessential for toxicity.

Altogether these results demonstrate that the average structure calculated in vacuo with NMR restraints remains essentially constant even when water molecules are added into the calculations.

Comparison of solid state (X-ray)/solution (NMR) structures: The RMSD between the rMD average structure (A7PHV) and the X-ray structure for the backbone is 0.72 Å, inclusive of the oxygens and the thioether bridge (Figure 4). This shows

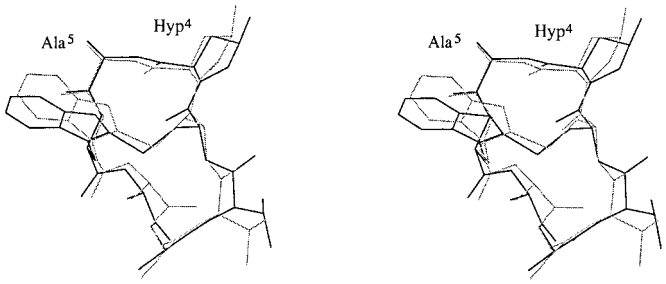

Figure 4. A stereoview of the backbone superposition of the [Ala^7]-phalloidin solid state structure (grey line) with the A7PHV rMD average molecular model (black line).

that the solution structure is quite close to that observed in the crystal state. A type I β-turn between the Cys^3-CO and the Trp^6-NH in the 15-membered ring 1 is present in both structures. The main difference is in the 18-membered ring 2 where the two consecutive γ-turns observed in the solid-state structure are not found in solution. This is very likely owing to the larger flexibility of the wider ring 2. In all cases the indole moiety points toward the Hyp^4–Ala^5 segment.

The superposition of [Ala^7]-phalloidin and phalloidin[13] rMD average molecular models (Figure 5) underlines similarities and differences between the two structures. The

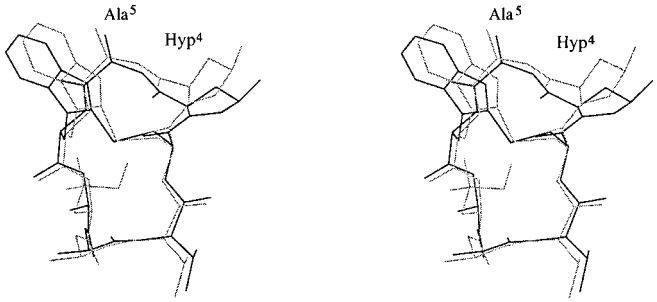

Figure 5. A stereoview of the backbone superposition of average molecular models: [Ala^7]-phalloidin (A7PHV, black line) and phalloidin[13] (grey line).

RMSD is 0.41 Å for the backbone atoms. In particular both structures present the same orientation of the indole ring and the occurrence of a type I β-turn between the Trp^6-HN and the Cys^3-CO. On the contrary the conformations of the Trp^6-Xxx^7 residues (Xxx = Leu in phalloidin and Ala in [Ala^7]-phalloidin) are substantially different.

Conclusion

In this study [Ala^7]-phalloidin, a toxic phalloidin synthetic derivative, has been investigated in the solid state by X-ray diffraction and in solution by NMR and MD methods.

The X-ray structure (at atomic resolution) represents as yet the first phallotoxin structure reported in the literature. First of all, the atropoisomerism of [Ala^7]-phalloidin can be unequivocally determined from the solid-state structure. By examination of the peptide chain clockwise, the sulfide bridge is above the main peptide ring.

The comparison of the solid state with the solution structures shows many similarities mainly in the Cys^3-Hyp^4-Ala^5-Trp^6 segment, where a type I β-turn occurs. In the X-ray structure, however, the Cys^3-Hyp^4-Ala^5-Trp^6 β-turn is also included in a α-turn (Cys^3–Ala^7), and, two consecutive γ-turns around the Ala^7 and the Ala^1 residues are observed. These structural motifs are not present in solution.

The Trp^6 indole ring orientation in the thioether bridge is the same in both solid state and solution structures, and points towards the Hyp^4–Ala^5 segment.

These findings indicate the relevance of the environment in the determination of the molecular conformations. The intramolecular hydrogen-bonding network, that stabilizes the molecular crystal structure, is partially destroyed in solution by the solvent. Noteworthy the [Ala^7]-phalloidin molecular model from the NMR data measured in DMSO is very similar to the natural phalloidin solution structure (RMSD 0.41 Å) determined by Kessler and Wein.[13] In the same solvent both molecules show a very rigid region (Cys^3–Trp^6) with the sulfide bridge and a more flexible part (Ala^7–D-Thr^2).

On these grounds we propose that the [Ala^7]-phalloidin structure represents a reliable reference scaffold for the phallotoxin family.

Experimental Section

Synthesis: Amino acids, chemicals, and solvents were of analytical grade. Analysis by thin-layer chromatography (TLC) was performed on precoated silica G-60 plates (Merck 60 F_{254}) using the solvent mixtures indicated for each substance. Spot detection was achieved by the ninhydrin reaction, iodine vapor staining or by the color reaction with cinnamaldehyde/HCl. The Kieselgel used for preparative separations was purchased from Merck. UV spectra were recorded on a Shimadzu UV2001PC spectrometer. CD spectra were measured on a Jasco J600 instrument with appropriate quartz cells. The crystalline diastereomer of L-3a-hydroxy-1,2,3,3a,8,8a-hexahydropyrrolo[2,3-*b*]indole-2-carboxylic acid (Hpi) was prepared according to Savige.[16] All linear peptides as well as monocyclic and bicyclic thioether peptides gave satisfactory amino acid analyses. The dipeptides H-*allo*-Hyp-Ala-O*t*Bu and Z-Ala-Ala-OH have been described elsewere.[19, 45] The binding affinity to F-actin was tested in the laboratory of Prof. H. Faulstich

at the Max Planck Institut für Medizinische Forschung, Ladenburg bei Heidelberg.

X-ray Diffraction: For crystallization [Ala^7]-phalloidin (40 mg) was dissolved in a hot mixture of ethanol/water 8:2. Crystals were formed after slow evaporation of the solvent at room temperature. Preliminary oscillation and Weissenberg photographs were taken to determine the crystal symmetry and the preliminary space group. The evaluation of cell constants was obtained by a least-square procedure on the angular settings of 25 reflections in the Θ range 21–25°. The crystallographic data are reported in Table 8. Data were measured on an Enraf–Nonius CAD-4 diffractometer equipped with graphite monochromated $Cu_{K\alpha}$ radiation ($\lambda = 1.5418$ Å).

Table 8. Crystal data and structure refinement for [Ala^7]-phalloidin.

empirical formula	$C_{32}H_{42}N_8O_9S$
formula weight	714.80
temperature [K]	293(2)
wavelength [Å]	1.54178
crystal system, space group	orthorhombic, $P2_12_12_1$
unit cell dimensions [Å]	$a = 10.468(3)$
	$b = 12.192(4)$
	$c = 27.350(3)$
volume [Å^3]	3491(2)
Z, ρ_{calcd} [Mg m^{-3}]	4, 1.360
absorption coefficient [mm^{-1}]	1.374
$F(000)$	1512
Θ range for data collection	3.23 to 69.99
reflections collected/unique	3731/3731
observed reflections [$I > 2\sigma(I)$]	3378
scan mode	$\omega - 2\Theta$
standard reflections	2
frequency of measurements [min]	60
intensity decay [%]	3
refinement method	full-matrix least-squares on F^2
data/restraints/parameters	3731/0/452
goodness-of-fit on F^2	1.040
final R indices [$I > 2\sigma(I)$]	$R1 = 0.0378$, w$R2 = 0.1109$
R indices (all data)	$R1 = 0.0437$, w$R2 = 0.1167$
largest diff. peak and hole [eA^{-3}]	0.183 and −0.282

The structure was solved by direct methods using the SIR 97 computer program.[46] Refinement was performed on F^2 (all data) by a full-matrix least-squares procedure, using SHELXL93.[47] All non-H atoms were refined with anisotropic displacement parameters

using a weighting Scheme with $w = 1/[\sigma^2(F_o^2)+(0.0739P)^2]$ where $P = (F_o^2+2F_c^2)/3$. The positions of the H-atoms were calculated with the exception of the hydrogen atoms of the OH and NH groups that were located in subsequent different Fourier analysis. During the refinement all hydrogen atoms were allowed to reside on their carrying atom, with U_{iso} set equal to 1.2 times (or 1.5 times for the methyl groups) the U_{eq} of the attached atom. The final unweighted R and wR factors on F^2, calculated on all data, were 0.044 and 0.117, respectively.

Atomic scattering factors for all atomic species were calculated from Cromer and Waber tables.[48] The final atomic parameters for all non-hydrogen atoms are reported in the supplementary material, the numbering of the atoms follows the recommendations of the IUPAC-IUB Commission[49] (Figure 6).

Crystallographic data (excluding structure factors) for the structure reported in this paper have been deposited with the Cambridge Crystallographic Data Centre as supplementary publication no. CCDC-147213. Copies of the data can be obtained free of charge on application to CCDC, 12 Union Road, Cambridge CB2 1EZ, UK (fax: (+44) 1223-336-033; e-mail: deposit@ccdc.cam.ac.uk).

NMR Measurements: [Ala^7]-Phalloidin was used as a 4.0×10^{-3} M solution in [D$_6$]DMSO (0.75 mL, Euriso Top, 100% isotopic purity). Proton spectra were recorded on a Varian Unity 400 operating at 400 MHz, located at the "Centro di Studio di Biocristallografia del C.N.R.", University of Naples

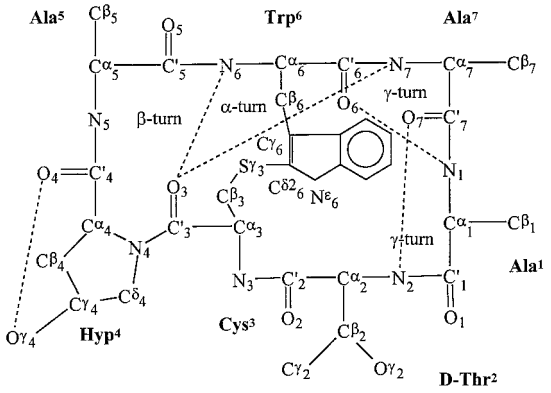

Figure 6. Schematic representation of intramolecular hydrogen bonds and secondary structure elements as observed by X-ray analysis. The dotted lines represent intramolecular hydrogen bonds.

"Federico II". Carbon spectra were acquired on a Bruker DRX operating at a carbon frequency of 100.6 MHz, located at the "Centro Interdipartimentale di Metodologie Chimico-Fisiche", University of Naples "Federico II". The spectra were acquired at 298 K. They were calibrated relative to [D$_6$]DMSO (^{1}H: $\delta = 2.50$, ^{13}C: $\delta = 39.5$) as an internal standard.

1D NMR spectra were recorded with 16 k data points and a spectral width of 5000 Hz. 2D NMR experiments, such as DQF-COSY, TOCSY, NOESY, and ROESY spectra were generally recorded with 2048 data points (4096 for the DQF-COSY) in $t2$ and 256 data points in $t1$, by the phase-sensitive States–Haberkorn method.[50] In both dimensions FIDs were multiplied by square-shifted sinebell weighting functions and data points were zero-filled to 1024 in $t1$ before Fourier transform. A spinlock mixing time (τ_m) of 80 ms, with a MLEV-17 sequence,[51] was used in the TOCSY spectra, and they were recorded in the temperature range 298–310 K for monitoring chemical shift changes with the temperature.

Two series of NOESY and ROESY spectra were acquired with mixing times of 50, 100, 200, 300, 400 ms and 60, 100, 160, 220 ms, respectively. Off-resonance effects, associated to the low-power spinlock field in ROESY spectra, were compensated by means of two π/2 hard pulses before and after the spinlock period.[52] NOE and ROE intensities were evaluated by integration of cross-peak volumes, by means of the appropriate VARIAN software.

The transformed 2D spectra were baseline corrected before measuring cross and diagonal peak volumes. The cross-peak volumes were normalized with respect to the diagonal peaks. The frequency offset effect in the rotating frame was also corrected.[52] The normalized volumes (A_i) give a linear build-up for short mixing time values up to 0.3 s. The cross-relaxation rates σ_{ij} were calculated from the slope of the build-up curves.[37] The same procedure was used for both NOESY and ROESY spectra.

Two separate lists of interproton distances from cross-relaxation rate values evaluated from NOESY (σ^N) and ROESY (σ^R) spectra were generated by Equation (1).

$$r_{ij} = r_{st}\,(\sigma_{st}/\sigma_{ij})^{1/6} \quad (1)$$

As a reference the Hyp^4–H$^{\beta\beta'}$ peak was chosen with the r_{st} interproton distance of 1.78 Å. An independent proof of the accuracy of the calibration was obtained by considering the cross peak between the Trp^6 indole NH proton and the H′$_7$ proton as standard reference with the r_{st} interproton distance of 2.82 Å.

^{13}C NMR spectra were recorded using a broad-band decoupling with 32 k data points, 45° read pulse, 0.73 s of acquisition time and a relaxation delay of 3.0 s. The spectral width was 220 ppm.

Carbon assignments were made with the aid of HMQC spectra, using a BIRD sequence for ^{12}CH presaturation,[53, 54] GARP decoupling during acquisition with 2048 data points in $t2$ and 256 increments in $t1$ (zero-filled to 512 before Fourier transform), a relaxation delay of 3 s and 128 scans per spectrum.

0947-6539/01/0707-1484 $ 17.50+.50/0 *Chem. Eur. J.* **2001**, *7*, No. 7

Structure calculations: Molecular dynamic simulations were performed on a Silicon Graphics INDIGO2 Workstation. The INSIGHT/DISCOVER (Biosym Technologies, San Diego, CA, USA) program with the consistent valence force field (CVFF)[55] was employed for energy minimizations (EM) and molecular dynamics (MD). The X-ray structure was taken as the starting model. This structure was relaxed by 500 steps of restrained conjugate gradients EM,[56, 57] imposing ROEs data as restraints on interproton distances.

The restrained molecular dynamics (rMD) simulation was performed in vacuo at 300 K with 0.5 fs time steps. The motion equation algorithm was of the leapfrog type.[58] The rMD simulation was carried out for 50 ps in the equilibration phase and or 160 ps without velocity rescaling; the temperature was kept constant at 300 K.

Interproton distances evaluated from ROE effects were inserted as restraints with a 10% tolerance during the simulations.[59] Pseudoatoms were used instead of protons not stereospecifically assigned.[60] Coordinates and velocities for the systems were dumped into a disk every 1000 steps. Data recorded during the last 50 ps of the simulation were used for the statistical analysis.

Acknowledgements

The authors thank Mrs. Suse Zobeley, (Max Planck Institut für Medizinische Forschung, Ladenburg bei Heidelberg, Germany) for the biological assays.

[1] T. Wieland, *Peptides of Poisonous Amanita Mushrooms*, Springer Verlag, New York, **1986**.
[2] F. Lynen, U. Wieland, *Liebigs Ann. Chem*. **1938**, *548*, 93–117.
[3] T. Wieland, K. Hannes, A. Schoepf, *Liebigs Ann. Chem*. **1958**, *617*, 152–162.
[4] T. Wieland, H. W. Schnabel, *Liebigs Ann. Chem*. **1962**, *657*, 218–225.
[5] H. Faulstich, O. Brodner, S. Walch, T. Wieland, *Liebigs Ann. Chem.* **1962**, *657*, 1218–1225.
[6] T. Wieland, H. Faulstich, *CRC Crit. Rev. Biochem.* **1978**, *5*, 185–260.
[7] H. Faulstich, A. J. Schaefer, M. Weckauf, *Hoppe Seyler's Z. Physiol. Chem.* **1977**, *358*, 181–184.
[8] P. Dancker, J. Low, W. Hasselbach, T. Wieland, *Biochim. Biophys. Acta* **1975**, *400*, 407–414.
[9] J. Low, P. Dancker, T. Wieland, *FEBS Lett.* **1975**, *54*, 263–265.
[10] J. De Vries, T. Wieland, *Biochemistry* **1978**, *17*, 1965–1968.
[11] D. J. Patel, A. E. Tonelli, P. Pfaender, H. Faulstich, T. Wieland, *J. Mol. Biol.* **1973**, *79*, 185–196.
[12] P. Boenzli, J. T. Gerig, *J. Am. Chem. Soc.* **1990**, *112*, 3719–3726.
[13] H. Kessler, T. Wein, *Liebigs Ann. Chem*. **1991**, 179–184.
[14] N. Kobayashi, S. Endo, H. Kobayashi, H. Faulstich, T. Wieland, *Eur. J. Biochem.* **1995**, *232*, 762–736.
[15] E. Munekata, N. Kobayashi, S. Endo, H. Faulstich, T. Wieland in *Peptide Chemistry 1990* (Ed.: Y. Shimonishi), Osaka, **1991**, pp. 333–338.
[16] W. E. Savige, *Aust. J. Chem.* **1975**, *28*, 2275–2287.
[17] W. E. Savige, A. Fontana, *J. Chem. Soc. Chem. Commun.* **1976**, 600–601.
[18] W. E. Savige, A. Fontana, *Int. J. Pept. Protein Res.* **1980**, *15*, 102–112.
[19] T. Wieland, T. Miura, A.Seeliger, *Int. J. Pept. Protein Res.* **1983**, *21*, 3–10.
[20] G. Zanotti, C. Birr, T. Wieland, *Int. J. Pept. Protein Res.* **1981**, *18*, 162–168.
[21] G. Zanotti, G. Petersen, T. Wieland, *Int. J. Pept. Protein Res.* **1992**, *40*, 551–558.
[22] T. Wieland, B. Beijer, A. Seeliger, J. Dabrowski, G. Zanotti, A. E. Tonelli, A. Gieren, B. Dederer, V. Lamm, E. Haedicke, *Liebigs Ann. Chem.* **1981**, 2318–2334.
[23] E. Benedetti in *Chemistry and Biochemistry of Amino Acids, Peptides and Proteins, Vol. 6* (Ed.: B. Weinstein), Marcel Dekker, New York, **1986**, pp. 105–184.
[24] E. Benedetti, G. Morelli, G. Nemethy, H. A. Scheraga, *Int. J. Pept. Protein Res.* **1983**, *22*, 1–15.
[25] V. Pavone, G. Gaeta, A. Lombardi, F. Nastri, O. Maglio, C. Isernia, M. Saviano, *Biopolymers* **1996**, *38*, 705–721.
[26] T. Ashida, M. Kakudo, *Bull. Chem. Soc. Jpn.* **1974**, *47*, 1129–1133.
[27] F. A. Momany, R. F. McGuire, A. W. Burgess, H. A. Scheraga, *J. Phys. Chem*. **1975**, *79*, 2361–2381.
[28] T. Takigawa, T. Ashida, Y. Sasada, M. Kakudo, *Bull. Chem. Soc. Jpn.* **1996**, *39*, 2369–2378.
[29] J. Janin, S. Wodak, M. Levitt, B. Maigret, *J. Mol. Biol.* **1978**, *125*, 357–386.
[30] C. Ramakrishan, N. Prasad, *Int. J. Pept. Protein Res.* **1971**, *3*, 209–231.
[31] L. Braunschweiler, R. R. Ernst, *J. Magn. Reson.* **1983**, *53*, 521–528.
[32] U. Piantini, O. W. Sørensen, R. R. Ernst, *J. Am. Chem. Soc.* **1982**, *104*, 6800–6801.
[33] M. Rance, O. W. Sørensen, G. Bodenhausen, G. Wagner, R. R. Ernst, K. Wüthrich, *Biochem. Biophys. Res. Commun.* **1983**, *117*, 479–485.
[34] A. A. Bothner-By, R. L. Stephens, J.-M. Lee, C. D. Warren, R. Jeanloz, *J. Am. Chem. Soc.* **1984**, *106*, 811–813.
[35] A. Bax, D. Davis, *J. Magn. Reson.* **1985**, *63*, 207–213.
[36] A. Kumar, G. Wagner, R. R. Ernst, K. Wüthrich, *J. Am. Chem. Soc.* **1981**, *103*, 3654–3658.
[37] D. Neuhaus, M. Williamson, *The Nuclear Overhauser Effect in Structural Conformation Analysis*, VCH, New York, **1989**.
[38] L. Mueller, *J. Am. Chem. Soc.* **1979**, *101*, 4481–4484.
[39] M. R. Bendall, D. T. Pegg, D. M. Doddrell, *J. Magn. Reson.* **1983**, *52*, 81–117.
[40] A. Bax, R. H. Griffey, B. L. Hawkins, *J. Magn. Reson.* **1983**, *55*, 301–315.
[41] K. Wüthrich, *NMR of Proteins and Nucleic Acids*, Wiley, New York, **1986**.
[42] C. Isernia, L. Paolillo, E. Russo, A. L. Pastore, G. Zanotti, S. Macura, *J. Biomol. NMR* **1992**, *2*, 573–582.
[43] V. F. Bystrov, *Prog. Nucl. Magn. Reson. Spectrosc.* **1976**, *10*, 41–82.
[44] G. D. Rose, L. M. Gierasch, J. A. Smith in *Advances in Protein Chemistry, Vol. 37* (Eds.: C. B. Anfisen, J. T. Edsael, F. M. Richards), Academic Press, Orlando, Florida, **1985**, pp. 1–109.
[45] M. Goodmand, R. Rupp, F. Nordes, *Bioorg. Chem.* **1961**, *1*, 294–297.
[46] A. Altomare, M. C. Burla, M. Camalli, G. Cascarano, G. Giacovazzo, A. Guagliardi, A. G. G. Moliterni, G. Polidori, R. Spagna, *SIR97 Program for Automatic Solution and Refinement of Crystal Structures*, University of Bari, Italy, **1997**.
[47] G. M. Sheldrick, *SHELXL 93*, *Program for Crystal Sructure Refinement*, University of Göttingen, Germany, **1993**.
[48] D. T. Cromer, J. T. Waber, *International Tables for X-Ray Crystallography, Vol. IV*, Kynoch Press (now distributed by D. Reidel Publ.) **1974**, Table 2.2 B.
[49] IUPAC-IUB Commission on Biochemistry Nomenclature in *Biochemistry* **1970**, *9*, 3471–3479.
[50] D. J. States, R. A. Haberkorn, D. J. Ruben, *J. Magn. Reson.* **1982**, *48*, 286–292.
[51] A. Bax, D. Davis, *J. Magn. Reson.* **1985**, *65*, 355–360.
[52] C. Griesinger, R. R. Ernst, *J. Magn. Reson.* **1987**, *75*, 261–271.
[53] A. Bax, S. Subramanian, *J. Magn. Reson.* **1986**, *67*, 565–569.
[54] R. A. Byrd, M. F. Summers, G. Zon, C. Spellmeyer Fouts, L. G. Marzilli, *J. Am. Chem. Soc*. **1986**, *108*, 504–505.
[55] S. Lifson, A. T. Hagler, P. Damber, *J. Am. Chem. Soc.* **1979**, *101*, 5111–5131.
[56] R. Fletcher, C. M. Reeves, *Comput. J.* **1964**, *7*, 149–154.
[57] W. F. van Gunsteren, M. Karplus, *J. Comput. Chem.* **1980**, *1*, 266–274.
[58] C. L. Brooks III, B. Montgomery Pettitt, M. Karplus, *Advances in Chemical Physics, Vol. LXXI*, Wiley, New York, **1988**, Chapter IV, pp. 33–37.
[59] W. F. van Gunsteren, H. J. C. Berendsen, *Angew. Chem.* **1990**, *102*, 1020–1055; *Angew. Chem. Int. Ed. Engl.* **1990**, *29*, 992–1023.
[60] K. Wüthrich, M. Billeter, W. Brown, *J. Mol. Biol.* **1983**, *169*, 949–961.

Received: July 14, 2000 [F2600]